The Property Nature of Fractal Disk Dimension: A Case Study of Poincare Sections of Harmonically Excited Pendulum.

T.A.O. Salau, Ph.D. and Ajide O. Olufemi, M.Sc.

Department of Mechanical Engineering, University of Ibadan, Nigeria.

E-mail: ooe.ajide@mail.ui.edu.ng

ABSTRACT

This study investigated whether or not that the fractal disk dimension is a property associable to Poincare section of harmonically excited pendulum. Five popular Runge-Kutta schemes (RK2, RK3, RK4, RK5, and RK6) were employed to simulate steady state Poincare sections for fixed drive frequency $\omega_D = 2/3$ and excitation period (T_D) based on time steps ($T_D/100 \le h \le T_D/1000$) at 2601 nodal points on the damp-forcing amplitude plane ($2.0 \le q \le 4.0$ and $0.9 \le g \le 1.5$) of the pendulum at 51×51 nodal points along each of q and g axis at equal intervals from initial condition (0.0).

Poincare sections validation was based on [1] result with further processing done by combination of disk count method and statistical analysis. The validation case result agreed qualitative well compared with [1]. Its estimated fractal disk dimension for schemes and constant time steps is 1.34 ± 0.03. The second order scheme recorded 14.2% deviation relative to mean (1.34) at time step ($h = T_p/100$), an indicator of its poor performance at larger time step due to its computational instability.

The schemes evaluated by their disk dimension absolute average percentage deviation relative to mean value ranks from best is RK4 or RK5, RK6, RK2 and RK3 with corresponding deviation results 10.0, 10.0, 10.1, 12.4 and 32.4. Thus third and second order schemes are the worst simulators and have to be used with care as they can lead to gross wrong estimate of fractal disk dimension. Although all schemes recorded large range deviation results an overall average absolute percentage deviations of 14.9 accommodating computation errors is a good indicator that fractal disk dimension is a property of Poincare section.

(Keywords**:** Poincare section, harmonically excited pendulum, Runge-Kutta schemes, fractal disk dimension)

INTRODUCTION

Fractal has been described as an object that displays self-similarity at various scales. According to [2], if any position of a fractal object is zoomed, we often noticed that the smaller section is actually a scale-down version of the big one. The concept of fractal nature is quintessential in nonlinear dynamics. Significant efforts have been made by researchers in the investigation of fractal nature of various nonlinear dynamic systems. The fractal nature of rock fracture surface developed under tension was examined by [3]. In the study, seven different rock samples were collected for the test. Variogram analysis (VA) and power spectral density (PSD) were employed in estimating fractal dimension. Fractal dimension results from PSD and VA indicated a well defined relationship for grain size and porosity. This finding is very useful in defining fractal properties of fracture surfaces that is sufficient for explaining rock fracture behavior.

Researchers [4] studied the fractal property of Lorenz attractor. The author successfully obtained explicit plots of the fractal structure of the Lorenz attractor using symbolic dynamics and multiple precision computations of periodic orbits. The author then applied Hausdorff dimension in the study of property nature of Lorenz attractor. The author's paper has provided useful information on the fractal characteristics of Lorenz attractor. [5] studied the fractal property of highway traffic data. From the results obtained, the fractal identification technique implies that there is a strong manifestation of fractal characteristics from the data collected. It is asserted in the paper that the fractal framework

has potential for description of observed data. The fractal property of the spatial distribution of acoustic emissions during the rock damage and failure process has been examined [6].Their research results showed significant variations in failure features for different parts of a specimen due to the structural variations in bedded rock salt. This study has provided a useful clue for forecasting the failure mode of bedded rock salt.

Other researchers [7] investigated the fractal nature of land forms. The paper adopted Variogram method and the cellular fractal model to estimate the fractal property of landforms in the Ordos block and surrounding areas. The authors' paper has satisfactorily demonstrated how fractal characteristics of landforms can be determined. More also, several other studies [8-14] corroborate the immense benefits of investigating the fractal properties of nonlinear dynamic systems. Fractal dimension is one of the most versatile tools for estimating fractal properties and has been a useful tool in various scientific fields [15]. Fractal dimension has been described by [16] as a ratio providing statistical index of complexity comparing how detail a fractal pattern changes with the scale at which it is measured. It has also been described as the space-filling capacity of a fractal. There is growing interest among researchers in the use of fractal dimension for nonlinear dynamics characterization.

In [17] article paper, fractal dimension was used to describe leaf complexity. Three hundred leaves from ten species were selected for the analysis. The authors remarked that well defined fractal dimension based features may be adopted to differentiate species with more than 90 % accuracy. The system response of a nonlinear harmonically driven pendulum has been studied using fractal dimension as a tool [18]. The study revealed that the numbers of nodes that have fractal dimension greater than 1.0 increase with increasing damping factor and decreasing forcing amplitude. As reported by the authors, the study result has potential application in the design of harmonically driven nonlinear engineering systems with a desired degree of chaotic response. The findings have practical application in engineering instruction in the areas of nonlinear dynamical systems. It also has useful application in aesthetic fashion design. [19] utilized fractal dimension to investigate the porosity of robot laser hardened specimens. The authors successfully developed a new technological process of hardening that is capable of decreasing the porosity of hardened specimen. Fractal dimension has also been found useful for investigating the microstructure of cement-base porous materials [20]. In the study, fractal dimensions of samples were determined from Zhang's model. The research finding shows the scale-dependent property of fractal dimensions of pore structures and the micro-fractal regions are identified for all collected samples. More interesting uses of fractal dimension for characterization have been illustrated [21-24].

Although very robust efforts have been made on the use of fractal dimension in nonlinear dynamics characterization, there is still a research gap. This study is motivated on the need to show that fractal disk dimension is a property of Poincare section of harmonically excited pendulum which must not vary significantly/drastically across the simulation schemes (RK2, RK3, RK4, RK5 and RK6). There is a strong conviction that the present paper research results will further enrich the literature on the choice of fractal dimension for fractal nature characterization of harmonically excited pendulum dynamics.

MATERIALS AND METHODS

This study adopted from [1] the non-dimensional and one dimensional governing equation of the damped, sinusoidally driven pendulum given by Equation (1). It is important to note that q is the damping quality parameter, g is the forcing amplitude, ω_D is the drive frequency and t represent time.

$$\frac{d^2\theta}{dt} + \frac{1}{q}\frac{d\theta}{dt} + \sin(\theta) = g\cos(\omega_D t) \qquad \textbf{(1)}$$

Simulation of Equation (1) with any of the Runge-Kutta schemes demands its transformation under the assumptions:

($\theta_1 = angular\ displacement$ and
$\theta_2 = angular\ velocity$)

to a pair of first order differential equations. Under these transformations Equations (2) and (3) are obtained.

$$\dot{\theta}_1 = \theta_2 \quad \textbf{(2)}$$

$$\dot{\theta}_2 = g\cos(\omega_D t) - \frac{1}{q}\theta_2 - \sin(\theta_1) \quad \textbf{(3)}$$

The present study utilized the popular constant operation time step second, third, fourth, fifth and the modified Butcher's (1964) fifth order Runge-Kutta schemes to simulate Equation (1) in its equivalent pair form given by the first order rate Equations (2) and (3). Researchers [25] provided details of each scheme, the corresponding summary of which are given in Equations (4) to (29) substituting $y \leftarrow \theta_1, \theta_2, x \leftarrow t$ and constant time step h.

Popular Second-Order Runge-Kutta Scheme (RK2)

The summarized popular second–order Runge-Kutta scheme is given by Equations (4) to (6) below:

$$y_{i+1} = y_i + (K_1 + K_2)h \quad \textbf{(4)}$$

$$K_1 = f(x_i, y_i) \quad \textbf{(5)}$$

$$K_2 = f(x_i + \frac{h}{2}, y_i + K_1\frac{h}{2}) \quad \textbf{(6)}$$

Popular Third-Order Runge-Kutta Scheme (RK3)

The summarized popular third–order Runge-Kutta scheme is given by Equations (7) to (10) below:

$$y_{i+1} = y_i + \frac{h}{6}\{K_1 + 4K_2 + K_3\} \quad \textbf{(7)}$$

$$K_1 = f(x_i, y_i) \quad \textbf{(8)}$$

$$K_2 = f(x_i + \frac{h}{2}, y_i + \frac{K_1 h}{2}) \quad \textbf{(9)}$$

$$K_3 = f(x_i + h, y_i - K_1 h + 2K_2 h) \quad \textbf{(10)}$$

Fourth-Order Runge-Kutta Scheme (RK4)

The summarized popular fourth–order Runge-Kutta scheme is given by Equations (11) to (15) below:

$$y_{i+1} = y_i + \frac{h}{6}\{K_1 + 2(K_2 + K_3) + K_4\} \quad \textbf{(11)}$$

$$K_1 = f(x_i, y_i) \quad \textbf{(12)}$$

$$K_2 = f(x_i + \frac{h}{2}, y_i + \frac{K_1 h}{2}) \quad \textbf{(13)}$$

$$K_3 = f(x_i + \frac{h}{2}, y_i + \frac{K_2 h}{2}) \quad \textbf{(14)}$$

$$K_4 = f(x_i + h, y_i + K_3 h) \quad \textbf{(15)}$$

Fifth-Order Runge-Kutta Scheme (RK5)

The summarized popular fifth–order Runge-Kutta scheme is given by Equations (16) to (22) below:

$$y_{i+1} = y_i + \frac{h}{90}\{7K_1 + 32K_3 + 12K_4 + 32K_5 + 7K_6\} \quad \textbf{(16)}$$

$$K_1 = f(x_i, y_i) \quad \textbf{(17)}$$

$$K_2 = f(x_i + \frac{h}{2}, y_i + \frac{K_1 h}{2}) \quad \textbf{(18)}$$

$$K_3 = f(x_i + \frac{h}{4}, y_i + \frac{(3K_1 + K_2)h}{16}) \quad \textbf{(19)}$$

$$K_4 = f(x_i + \frac{h}{2}, y_i + \frac{K_3 h}{2}) \quad \textbf{(20)}$$

$$K_5 = f(x_i + \frac{3h}{4}, y_i + \frac{(-3K_2 + 6K_3 + 9K_4)h}{16}) \quad \textbf{(21)}$$

$$K_6 = f(x_i + h, y_i + \frac{(K_1 + 4K_2 + 6K_3 - 12K_4 + 8K_5)h}{7}) \quad \textbf{(22)}$$

Modified Butcher's (1964) Fifth-Order Runge-Kutta Scheme (RK6)

The summarized popular modified Butcher's (1964) fifth–order Runge-Kutta scheme is given by Equations (23) to (29) below:

$$y_{i+1} = y_i + \frac{h}{90}\{7K_1 + 32K_3 + 12K_4 + 32K_5 + 7K_6\} \quad \textbf{(23)}$$

$$K_1 = f(x_i, y_i) \quad \textbf{(24)}$$

$$K_2 = f(x_i + \frac{h}{4}, y_i + \frac{K_1 h}{4}) \quad \textbf{(25)}$$

$$K_3 = f(x_i + \frac{h}{4}, y_i + \frac{(K_1 + K_2)h}{8}) \quad \textbf{(26)}$$

$$K_4 = f(x_i + \frac{h}{2}, y_i - \frac{K_2 h}{2} + K_3 h) \quad \textbf{(27)}$$

$$K_5 = f(x_i + \frac{3h}{4}, y_i + \frac{(K_1 + 9K_4)h}{16}) \quad \textbf{(28)}$$

$$K_6 = f(x_i + h, y_i + \frac{(-3K_1 + 2K_2 + 12K_3 - 12K_4 + 8K_5)h}{7}) \quad \textbf{(29)}$$

Study Parameters

In tune with literature research interest, this study focuses on the parameter plane defined by $2.0 \le q \le 4.0$ and $0.9 \le g \le 1.5$, fixed drive frequency $\omega_D = \frac{2}{3}$, and ten fixed simulation time steps selected uniformly between $\frac{T_D}{100} \le h \le \frac{T_D}{1000}$ for $T_D = \frac{2\pi}{\omega_D}$.

A total of 2601 nodal points cases were investigated according to 51×51 nodal points along each of q and g axis at equal intervals. The initial conditions for all studied cases is (0,0) and the simulation was executed for 2010-excitation periods including 10-periods of transient and 2000-peiods of steady solutions.

The associated Poincare sections were investigated for their space filling ability using fractal disk dimension characterization [26]. Ten systematic observation scales of disk size variation and quantity of disks required for complete covering of the corresponding Poincare section were made using generation seed value of 9876. This process enables the determination of 'optimum' number of disks required at specified observation scale.

RESULTS AND DISCUSSION

The core of the present study is simulation and fractal characterization of Poincare section using Runge-Kutta schemes and disk count method in conjunction with statistical analysis. Therefore, a typical Poincare section is provided in Figure 1. The procedure for estimating its corresponding fractal disk dimension is given by Table 1 and Figure 2.

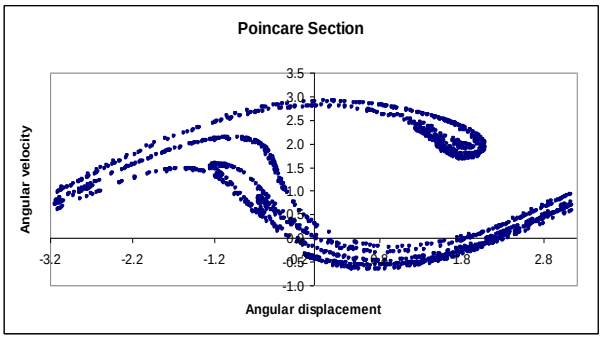

Figure 1: A Typical Poincare Section of the Harmonically Excited Nonlinear Pendulum simulated with RK4 for g =1.5, q =4.0 and $h = T_p/500$.

The Poincare section in Figure 1 compare qualitatively well with [1] result and has an estimated fractal disk dimension of 1.37 as demonstrated via Table 1 and Figure 2.

Table 1: Variation of disk counted (Y) with observation scale (X) for Poincare section simulated with RK4 for g =1.5, q =4.0 and $h = T_p/500$.

Scale (X)	1.00	2.00	3.00	4.00	5.00	6.00	7.00	8.00	9.00	10.00
Disk counted (Y)	2.00	5.00	8.00	13.00	17.00	21.00	27.00	32.00	41.00	48.00
Log(X)	0.00	0.69	1.10	1.39	1.61	1.79	1.95	2.08	2.20	2.30
Log(Y)	0.69	1.61	2.08	2.56	2.83	3.04	3.30	3.47	3.71	3.87

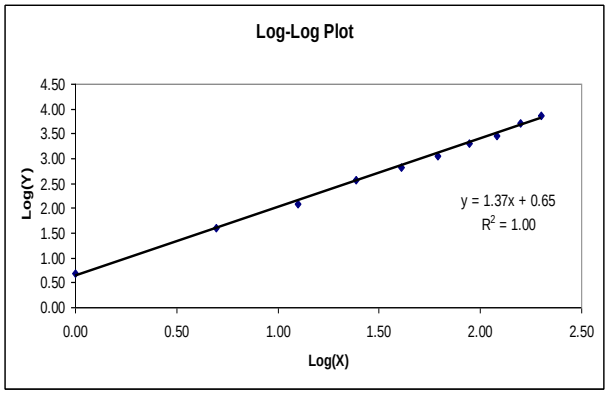

Figure 2: Log-Log Plot of Observation Scale versus Disk Counted for Poincare Section simulated with RK4 for g =1.5, q =4.0 and $h = T_p/500$.

Figure 2 shows there is a linear trend to the Log-Log plot of variation of observation scale versus disk counted with a slope of 1.37 corresponding to the fractal disk dimension estimate of the Poincare section obtained for g =1.5 and q =4.0 when the simulation is effected with the fourth order Runge-Kutta scheme.

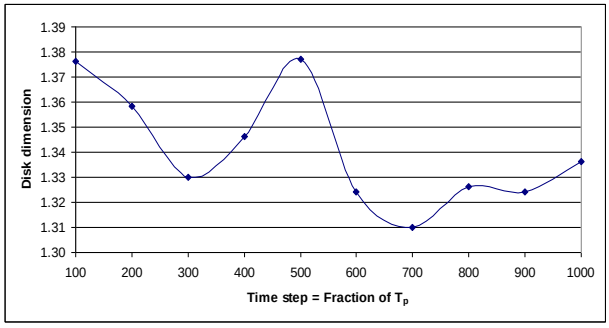

Figure 3: Variation of the Fractal Disk Dimension of Poincare Section with simulation time step using RK4 with g =1.5, q =4.0 and $h = T_p/500$.

Figure 3 shows the estimated fractal disk dimension of the Poincare section varies insignificantly within 1.35 ± 0.02 for the studied constant time steps selected from $T_p/100 \le h \le T_p/1000$.

Figure 4 refers to the variation of the simulation schemes. Here again the estimated fractal disk dimension of the Poincare section varies insignificantly within 1.35 ± 0.02 for the studied Runge-Kutta schemes.

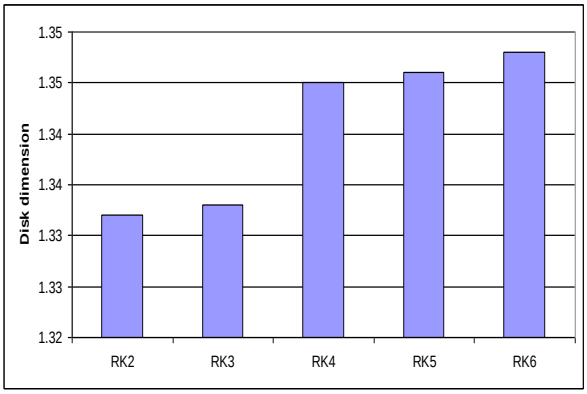

Figure 4: Variation of the fractal disk dimension of Poincare section with simulation schemes for g =1.5, q =4.0 and $h = T_P/500$.

Because the estimated fractal disk dimension of the Poincare section varies insignificantly with simulation time steps and schemes is suggestive that it can be taken to be a property. The results obtained for the verification of the reliability and consistence of this claim for large number of different selected g and q combinations are presented in the subsequent sections.

Table 2 shows the mean value of the estimated fractal disk dimension across the schemes and the entire studied constant time steps is 1.34 with a standard deviation of ± 0.03.

Table 2: Variation of Estimated Fractal Disk Dimension with Schemes and Time Steps for g =1.5, q =4.0.

Time step=Fraction of T_p	Estimated fractal disk dimension by scheme				
	RK2	**RK3**	**RK4**	**RK5**	**RK6**
100	1.15	1.36	1.38	1.38	1.36
200	1.35	1.37	1.32	1.36	1.37
300	1.37	1.36	1.36	1.38	1.34
400	1.33	1.33	1.36	1.33	1.34
500	1.36	1.33	1.35	1.35	1.37
600	1.33	1.32	1.37	1.37	1.33
700	1.35	1.34	1.34	1.33	1.33
800	1.36	1.36	1.33	1.35	1.36
900	1.34	1.34	1.32	1.36	1.32
1000	1.32	1.36	1.37	1.34	1.32
MDD	1.33	1.35	1.35	1.35	1.34
STD	0.06	0.02	0.02	0.02	0.02

Note: MDD = mean value of the estimated fractal disk dimension across schemes and STD =

Table 3: Selected Cases of Variation of the Estimated Fractal Disk Dimension of Poincare Section with Simulation Schemes using Constant Time Step ($h = T_P/500$).

Parameters		**Estimated Dimension by Scheme**				
g	q	**RK2**	**RK3**	**RK4**	**RK5**	**RK6**
0.900	2.000	0.00	0.00	0.00	0.00	0.00
0.912	3.920	1.20	1.24	1.23	1.21	1.24
0.936	3.840	0.46	0.50	0.47	0.46	0.49
0.960	3.760	0.00	0.00	0.00	0.00	0.00
0.984	3.680	0.29	0.13	0.60	0.69	0.62
1.008	3.600	0.49	0.38	0.49	0.49	0.49
1.032	3.520	0.94	0.35	0.98	0.93	0.93
1.056	3.440	0.64	0.41	0.64	0.63	0.63
1.080	3.360	0.36	0.21	0.40	0.36	0.33
1.104	3.280	1.00	0.84	1.03	0.96	0.99
1.128	3.200	1.20	1.17	1.20	1.17	1.20
1.152	3.120	0.99	0.94	0.54	1.02	0.97
1.176	3.040	1.18	1.17	1.17	1.18	1.18
1.200	2.960	1.16	1.18	1.18	1.18	1.18
1.224	2.880	1.15	1.16	1.14	1.16	1.20
1.248	2.800	1.16	1.15	1.14	1.14	1.15
1.272	2.720	1.15	0.66	1.14	1.16	1.13
1.296	2.640	1.13	1.10	1.12	1.13	1.12
1.320	2.560	1.13	1.10	1.11	1.12	1.11
1.344	2.480	1.11	1.09	1.11	1.13	1.15
1.368	2.400	1.10	1.06	1.09	1.09	1.10
1.392	2.320	1.09	0.32	1.08	1.11	1.11
1.416	2.240	0.43	0.22	0.43	0.48	0.48
1.440	2.160	1.06	1.09	1.14	1.07	1.08
1.464	2.080	0.12	0.49	0.78	0.89	0.79
1.488	2.000	0.00	0.30	0.41	0.41	0.41
1.500	3.960	1.35	1.36	1.32	1.33	1.35
1.500	4.000	1.33	1.33	1.35	1.35	1.35

Table 4: Selected Cases of Variation of Absolute Percentage Deviation of the Estimated Fractal Disk Dimension of Poincare Section Relative to the Mean Value for all Simulation Schemes using Constant Time Step ($h = T_P/500$).

Parameters				Absolute percentage deviation of the estimated fractal disk dimension relative to the mean value by scheme				
g	q	MDD	STD	RK2	RK3	RK4	RK5	RK6
0.900	2.000	0.00	0.00	0.0	0.0	0.0	0.0	0.0
0.912	3.920	1.22	0.02	1.8	1.6	0.2	1.2	1.2
0.936	3.840	0.48	0.02	2.7	5.3	1.7	3.2	2.3
0.960	3.760	0.00	0.00	0.0	0.0	0.0	0.0	0.0
0.984	3.680	0.46	0.22	37.5	72.6	29.0	48.2	32.9
1.008	3.600	0.47	0.04	5.6	18.3	4.3	4.3	4.3
1.032	3.520	0.83	0.24	13.8	57.2	18.8	11.9	12.7
1.056	3.440	0.59	0.09	7.8	30.4	8.3	6.6	7.6
1.080	3.360	0.33	0.06	8.7	36.0	19.6	8.7	1.0
1.104	3.280	0.96	0.06	3.7	12.7	6.4	0.3	2.9
1.128	3.200	1.19	0.01	0.5	1.2	1.2	1.6	1.0
1.152	3.120	0.89	0.18	10.7	5.6	39.3	14.2	8.8
1.176	3.040	1.18	0.01	0.2	0.8	0.3	0.7	0.2
1.200	2.960	1.18	0.01	1.0	0.5	0.0	0.1	0.5
1.224	2.880	1.16	0.02	0.7	0.5	1.9	0.2	3.3
1.248	2.800	1.15	0.01	1.0	0.5	0.8	0.8	0.1
1.272	2.720	1.05	0.19	9.4	36.9	9.2	10.4	7.9
1.296	2.640	1.12	0.01	1.1	1.6	0.1	0.6	0.2
1.320	2.560	1.11	0.01	1.6	1.2	0.3	0.1	0.1
1.344	2.480	1.12	0.02	0.6	2.2	0.9	0.7	2.9
1.368	2.400	1.09	0.01	1.0	2.6	0.3	0.3	1.1
1.392	2.320	0.94	0.31	16.0	65.6	14.9	17.4	17.4
1.416	2.240	0.41	0.10	5.1	47.0	6.1	17.9	17.9
1.440	2.160	1.09	0.03	2.1	0.3	4.5	1.7	1.0
1.464	2.080	0.62	0.28	79.9	20.2	26.4	45.1	28.7
1.488	2.000	0.31	0.16	100.0	3.1	34.4	34.4	34.4
1.500	3.960	1.34	0.01	0.4	1.6	1.4	0.9	0.4
1.500	4.000	1.34	0.01	0.7	0.6	0.3	0.4	0.5
			Average	11.2	15.2	8.2	8.3	6.8

Note: MDD = mean value of the estimated fractal disk dimension across scheme and STD = corresponding standard deviation.

The estimated fractal disk dimension prescribed by second order Runge-Kutta at constant time step ($h = T_P/100$) deviated from the global mean value (1.34) by absolute value of 14.2% , an indication of possible poor result associated with larger step and scheme computational instability.

Referring to Table 3, the frequency of large absolute deviation of the estimated fractal disk dimension prescribed by third order Runge-Kutta scheme compare with the remaining four schemes is 32.1% on the average. This is a suggestive indicator that third order scheme is inadequate for the purpose of simulation and further characterization of Poincare section when higher accuracy is desirable.

Table 4 shows the average of the absolute percentage deviation of the estimated fractal disk dimension relative to the mean for RK2, RK3, RK4, RK5, RK6 are respectively 11.2,15.2, 8.2, 8.3 and 6.8.

However, similar analysis for expanded total cases of 2601 selected at constant step at 51×51 nodal points along each of the parameter axes supported the best rank of the schemes as RK4 or RK5, RK6, RK2 and RK3. The corresponding respective average percentage deviation is 10.0, 10.0, 10.1, 12.4 and 32.4. In conclusion, both the selected results and the comprehensive results marked third order scheme as the worst simulator.

In view of this, its use for simulation of the Poincare section of nonlinear harmonically excited pendulum must be with care as it can lead to gross wrong estimation of associated fractal disk dimension. Further reference to Table 4 shows that the range of absolute percentage deviation of the estimated fractal disk dimension relative to the mean value for RK2, RK3, RK4, RK5, RK6 are respectively (0.0-100.0), (0.0-72.6), (0.0-39.3), (0.0-48.2) and (0.0-34.4) while the corresponding average of the absolute percentage deviation across the selected cases are 11.2, 15.2, 8.2, 8.3, 6.8. However, the average of the absolute percentage deviation across the selected cases and schemes is 9.9. It is to be noted that both second and third order schemes suffered larger range and average, another possible indicator that these schemes are poor Poincare section simulators.

For all the 2601 nodes investigated, the range of absolute percentage deviation of the estimated fractal disk dimension relative to the mean value for RK2, RK3, RK4, RK5, RK6 are respectively (0.0-400.0), (0.0-400.0), (0.0-400.0), (0.0-150.0) and (0.0-241.1) while the corresponding average of the absolute percentage deviation across the selected cases are 12.4, 32.0, 10.0, 10.0, 10.1. In addition, the average of the absolute percentage deviation across the selected cases and schemes is 14.9. Here again the larger range and average of absolute percentage deviation recorded by second and third order schemes is a re-affirmation of their inaccuracy as Poincare section simulators. It is important to note that despite relative large range values recorded by all the schemes an average absolute percentage deviation of 14.9 is a good indicator pointing to fractal disk dimension as an entity property of Poincare section.

Figures 5, 6 and 7 provided further illumination of the property nature of the fractal disk dimension measurement. The distribution of the normalized frequency of the standard deviation (STD) of the estimated fractal disk dimension across schemes and for 2601 cases is given by Figure 5 in which bias is strong for lower standard deviation.

In addition, Figures 6 and 7-(a zoom up of Figure 6) shows that there is a qualitative agreement of the estimated fractal disk dimension distribution for all the schemes. The relative degree of computation instability associated with individual scheme can be used to account for the quantitative differences recorded between the schemes.

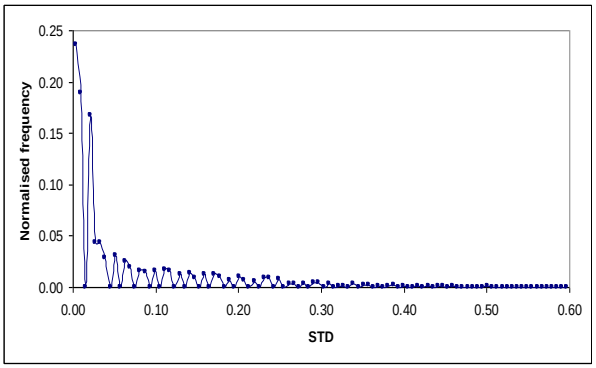

Figure 5: Normalized Frequency Distribution of the Standard Deviation (STD) of Estimated Fractal Disk Dimension of Poincare Sections with simulation time step $h = T_P/500$ using all schemes and with $2.0 \le q \le 4.0$ and $0.9 \le g \le 1.5$.

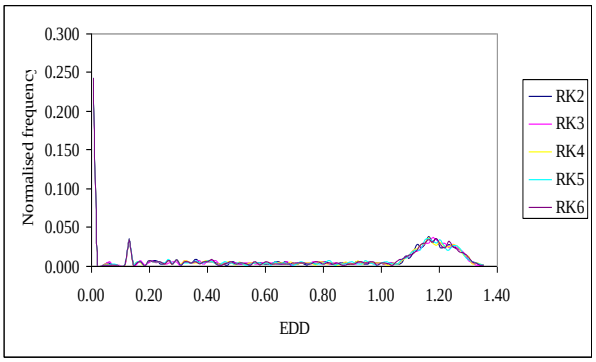

Figure 6: Normalized Frequency Distribution of the Estimated Fractal Disk Dimension (EDD) of Poincare Sections with simulation time step $h = T_P/500$ using all schemes and with $2.0 \le q \le 4.0$ and $0.9 \le g \le 1.5$.

Referring to Figures 8, 9 and Table 5: there is visual agreement between the figures and there corresponding coefficient of fitness. The higher coefficient of fitness (R^2=0.99) and slope value that is not less than 0.99 recorded between pair of scheme from RK4, RK5 and RK6 are strong indicator that any of these schemes is acceptable as good simulator of Poincare section with further processing or not.

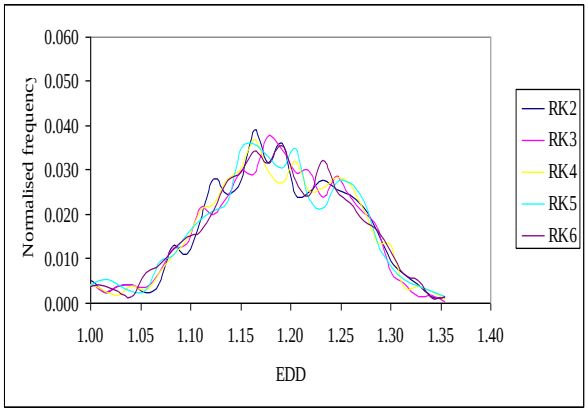

Figure 7: Zoomed-up Normalized Frequency Distribution of the Estimated Fractal Disk Dimension (EDD) of Poincare Sections with simulation time step $h = T_P/500$ using all schemes and with $2.0 \le q \le 4.0$ and $0.9 \le g \le 1.5$.

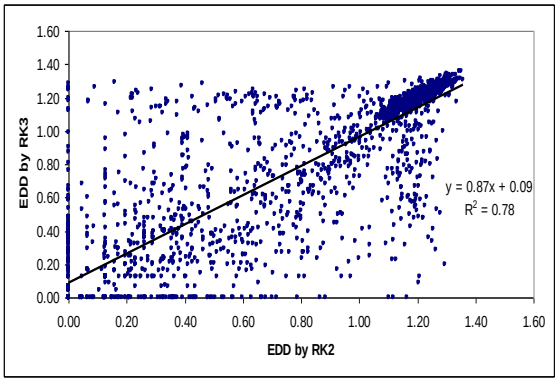

Figure 8: Correlation Plot of the Estimated Fractal Disk Dimension (EDD) by RK2 and RK3 with simulation time step $h = T_P/500$ and $2.0 \le q \le 4.0$ and $0.9 \le g \le 1.5$.

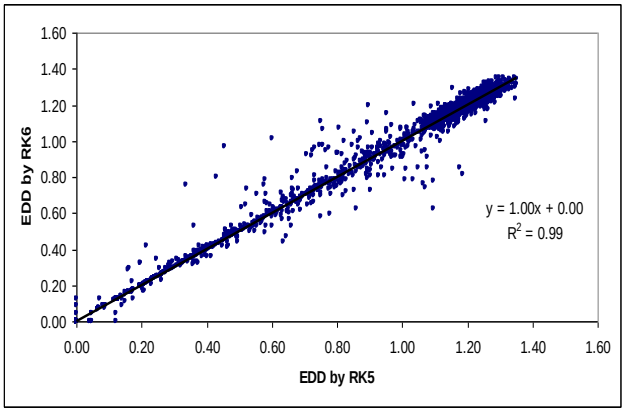

Figure 9: Correlation Plot of the Estimated Fractal Disk Dimension (EDD) by RK5 and RK6 with simulation time step $h = T_P/500$ and $2.0 \le q \le 4.0$ and. $0.9 \le g \le 1.5$

CONCLUSION

This study has shown with the aid of five popular Runge-Kutta schemes and fractal disk count analysis in conjunction with statistical analysis that Poincare section (attractor entity) of harmonically excited nonlinear pendulum has fractal disk dimension property. The trade-off in the estimated fractal disk dimensions of the attractor Poincare are justified with the potential computational error associated with individual scheme due to their relative theoretical and computational instabilities. However, this study strongly recommended any of the fourth, fifth and the modified Butcher's (1964) fifth order schemes for simulation of Poincare section whenever higher result accuracy is desired.

Table 5: Trend-line Parameters for Correlation Plot of the Estimated Fractal Disk Dimension (EDD) between selected pair of Runge-Kutta Schemes with simulation time step $h = T_P/500$ and $2.0 \le q \le 4.0$ and $0.9 \le g \le 1.5$.

	Trend line parameters		
Paired Scheme	**Slope**	**Intercept**	**Coefficient of fitness (R^2)**
RK2 versus RK3	0.87	0.09	0.78
RK2 versus RK4	0.98	0.02	0.96
RK2 versus RK5	0.97	0.02	0.95
RK2 versus RK6	0.98	0.02	0.95
RK3 versus RK4	0.88	0.08	0.77
RK3 versus RK5	0.88	0.08	0.77
RK3 versus RK6	0.88	0.08	0.77
RK4 versus RK5	0.99	0.00	0.99
RK4 versus RK6	0.99	0.01	0.99
RK5 versus RK6	1.00	0.00	0.99

REFERENCES

1. Gregory, L.B. and P.G. Jerry. 1990. *Chaotic Dynamics: An Introduction*. Cambridge University Press: Boston, MA. 3-5 & 40-75.

2. Juan, L.M. 2007. "The Nature of Fractals." *Third Apex to Fractovia*. www.fractovia.org

3. Babadagli, T. and K. Develi. 2003. "Fractal Characteristics of Rocks Fractured Under Tension". *Theoretical and Applied Fracture Mechanics*. 39:73-88.

4. Divakar, V. 2004. "The Fractal Property of the Lorenz Attractor". *Physica D*.190:115-128.

5. Pengjiang S., W. Meng, and K. Santi. 2007. "Fractal Nature of Highway Traffic Data". *Computers and Mathematics with Applications*. 54:107-116.

6. Xie, H.P., J.F. Liu, Y. Ju, J. Li and L.Z. Xie. 2011. "Fractal Property of Spatial Distribution of Acoustic Emissions During the Failure Process of Bedded Rock Salt". *International Journal of Rock Mechanics & Mining Sciences*.48:1344-1351.

7. Lisi, B., H. Honglin, W. Zhanyu, and S. Feng. 2012. "Fractal Properties of Landform in the Ordos Block and Surrounding Areas". *China. Geomorphology*. 175-176, 151-162.
8. Meifeng, D. and T. Lixin. 2005. "Fractal Properties of Refined Box Dimension on Functional Graph". *Chaos, Solitons and Fractals*. 23:1371-1379.

9. Ceylan, S. 2006. "Fractal Properties of Earthquakes in Marmara". *Journal of Istanbul Kuthur University*. 99-108.

10. Maricel, A., I. Paulos, N. Petra, R. Cristina, A. Adrian, and V. Petre. 2004. "Fractal Characteristics of the Solidification Process". *Materials Transaction*. 45(3):972-975.

11. Xianju, J., L. Bei, T. Ye, J. Nanguo, and D. An. 2013. "Study on Fractal Characteristics of Cracks and Pore Structure of Concrete Based on Digital Image Technology". *Research Journal of Applied Sciences, Engineering and Technology*. 5(11):3165-3171.

12. Tang, S. 1999. "Prediction of Fractal Properties of Polystyrene Aggregates". *Colloids and Surfaces A: Physicochemical and Engineering Aspects*. 157:185-192.

13. Guillermo, A., A.C. Hilda, and B. Carlo. 1999. "Fractal Properties of DNA Walks". *Biosystems*. 49:63-70.

14. Bitter, A., R. Dover, and Y. Shai. 2012. "Fractal Properties of Macrophanage Membrane Studied by AFM". *Micron*. 43:1239-1245.

15. James, T. 1989. "Estimating Fractal Dimension". *J. Opt. Soc. Am. A.* 7:1055-1073.

16. Wikipedia. 2013. "Fractal Dimension". Wikimedia Foundation Inc.

17. Borkowski, W. 1990. "Fractal Dimension Based Features are Useful Descriptions of Leaf Complexity and Shape". *Can.J. for Res.* 29:1301-1310.

18. Salau, T.A.O. and A.A. Olabode. 2013. "Fractal Characterization and Iso-Mapping of Parameter Plane of Harmonically Excited Pendulum". *International Journal of Scientific and Engineering Research (IJSER)*. 7(7):790-797.

19. Matej, B., P. Peter, K. Peter, Z. Milan, B. Igor, and V. Timotej. 2013. "Using Fractal Dimensions for Determination of Porosity of Robot Laser Hardened Specimens". *International Journal of Computer Sciences Issues*. 10, (2-3):184-190.

20. Qiang, Z., L. Mingyong, P. Xiaoyun, L. Le, and L. Kefei. 2013. "Surface Fractal Dimension. An Indicator to Characterize the Microstructure of Cement Based Porous Materials". *Applied Surface Science*. 282:302-307.
21. Chen, S.G. 1992. "Fractal Dimension of Correlation Clusters for Conformal Fields". *Communication Theory Physics*. 17(2):239-242.

22. Robert, C.M. and P.L. John. 1993. "Fractal Dimension and Nonlinear Dynamical Processes". *SPIE Proceedings, Chaos in Communication* 2038:342.

23. Ogawa, S., P. Baveye, W.B. Charles, J. Parlange, and T. Steenhuis. 1999. "Surface Characteristics of Preferential Flow Patterns in Field Soils: Evaluation and Effect of Image Processing". *Geoderma*. 88:109-136.

24. Ding, W. 2012. "Fractal Dimension Features of Soil Features of Soil Aggregates Distribution with the Different Reclamation Years on Loess Plateau". *Sensor Letters*. 10(1-2):555-561.

25. Steven, C.C. and P.C. Raymond. 2006. *Numerical Methods for Engineers. Fifth edition*. McGraw-Hill: New York, NY. ISBN 007-124429-8.

26. Salau, T.A.O. and O.O. Ajide. 2012. "Disk and Box Dimensions: Selected Case Studies of Fractals with IFS Codes". *International Journal of Sciences and Technology (IJST)*. 1(5):234-247.

ABOUT THE AUTHORS

Dr. SALAU Tajudeen Abiola Ogunniyi, is a Senior Lecturer in the department of Mechanical of Engineering, University of Ibadan, Nigeria. He joined the services of the University of Ibadan in February 1993 as Lecturer 2 in the department of Mechanical Engineering. He was promoted to Lecturer 1 in 2002 and Senior Lecturer in 2008.He had served the department in various capacities. He was the Coordinator of the Department for 2004/2005 and 2005/2006 academic sessions. He was the recipient of M.K.O Abiola postgraduate scholarship in 1993/1994 session while in his Ph.D. research program in the University of Ibadan. Dr. Salau has many publications in learned journals and international conference proceedings especially in the area of nonlinear dynamics. He had served as external examiner in Departments of Mechanical Engineering of some institutions of higher learning in the country and a reviewer/rapporteur in some reputable international conference proceedings. His area of specialization is solid mechanics with bias in nonlinear dynamics and chaos. Dr. Salau is a corporate member, Nigerian Society of Engineers (NSE). He is a registered Engineer by the Council for Regulations of Engineering in Nigeria (COREN). He is happily married and blessed with children.

Engr. AJIDE Olusegun Olufemi, is currently a Lecturer 2 in the Department of Mechanical Engineering, University of Ibadan, Nigeria. He joined the services of the University of Ibadan on 1st December 2010 as Lecturer 2. He had worked as the Project Site Engineer/Manager of PRETOX Engineering Nigeria Ltd., Nigeria. Ajide obtained B.Sc. (Hons.) in 2003 from the Obafemi Awolowo University, Nigeria and M.Sc. in 2008 from the University of Ibadan, Nigeria. He received the prestigious Professor Bamiro Prize (Vice Chancellor Award) in 2008 for the overall best M.Sc. student in Mechanical Engineering (Solid Mechanics), University of Ibadan, Nigeria. He has some publications in learned journals and conference proceedings. His research interests are in area of Solid Mechanics, Applied Mechanics and Materials Engineering. Engr. Ajide is a COREN registered Engineer. He is a corporate member of the Nigerian Society of Engineers (NSE) as well as corporate member of the Nigerian Institution of Mechanical Engineers (NIMechE).

SUGGESTED CITATION

Salau, T.A.O. and A.O. Olufemi. 2014. "The Property Nature of Fractal Disk Dimension: A Case Study of Poincare Sections of Harmonically Excited Pendulum". *Pacific Journal of Science and Technology*. 15(1):13-23.

Pacific Journal of Science and Technology